ADVANCED MATERIALS

DOI: 10.1002/adma.200600797

Organic Solar Cells Using Transparent SnO_2–F Anodes**

By *Fan Yang* and *Stephen R. Forrest**

Organic solar cells have attracted attention as a means to achieve low-cost solar-energy conversion owing to their ease of manufacture and compatibility with flexible substrates.[1,2] Conventional organic molecular photovoltaic (PV) devices and light-emitting diodes (OLEDs) are typically grown on transparent indium tin oxide (ITO) anodes[3] that are also widely used for flat-panel displays (FPDs). The scarcity of In, along with the rapid expansion of FPD production, has resulted in a soaring price of ITO-coated glass substrates, with the current price up to ten times greater than in 2003.[4] Alternative transparent conducting oxides such as doped SnO_2 or ZnO have been used as electrodes in dye-sensitized,[5] CdTe,[6] microcrystalline Si, and amorphous Si PV devices.[7] Organic small-molecule or polymeric devices, with active layers typically <1000 Å thick, can readily be shorted owing to the pronounced surface-roughness characteristic of these oxide variants. Nevertheless, the cost of F-doped SnO_2 (SnO_2–F)-coated glass is less than one third that of ITO-coated glass.[8] While there have been reports of using SnO_2–F as the transparent anode for polymeric OLEDs[9,10] and solar cells,[11,12] to our knowledge there has yet to be a demonstration of an organic heterojunction (HJ) PV cell based on SnO_2–F anodes with an efficiency greater than 0.1 %.[11,12]

Here, we report on copper phthalocyanine (CuPc)/C_{60} HJ PV cells on SnO_2–F anodes[8] with a power conversion efficiency of 2.5 % at 1 sun simulated AM 1.5 G (AM: air mass; G: Global) illumination. The organic layers were grown by organic vapor-phase deposition (OVPD)[13,14] that enabled complete coverage of the rough oxide surface, effectively preventing shorts between opposing cathode and anode contacts. In addition, we show that by controlling the organic-film morphology, we can grow the donor–acceptor (D–A) interface into a three-dimensional interdigitated bulk HJ (BHJ) structure, resulting in power-conversion efficiencies nearly twice those of analogous devices with a planar heterointerface.

As shown in Figure 1a, the 750 nm thick SnO_2–F-coated glass substrates have 70–80 % transmittance in the visible range, or approximately 10 % less than that for glass with 150 nm thick ITO coatings. The absorption of both substrates has a high-energy cutoff at wavelengths less than 350 nm, implying a match of the transparency window to that of the solar radiation spectrum.[15] The sheet resistance of SnO_2–F-coated glass is less than 12 Ω/sq.,[8] lower than that of ITO-coated glass (15 Ω/sq.)[16] The high transparency and small resistance

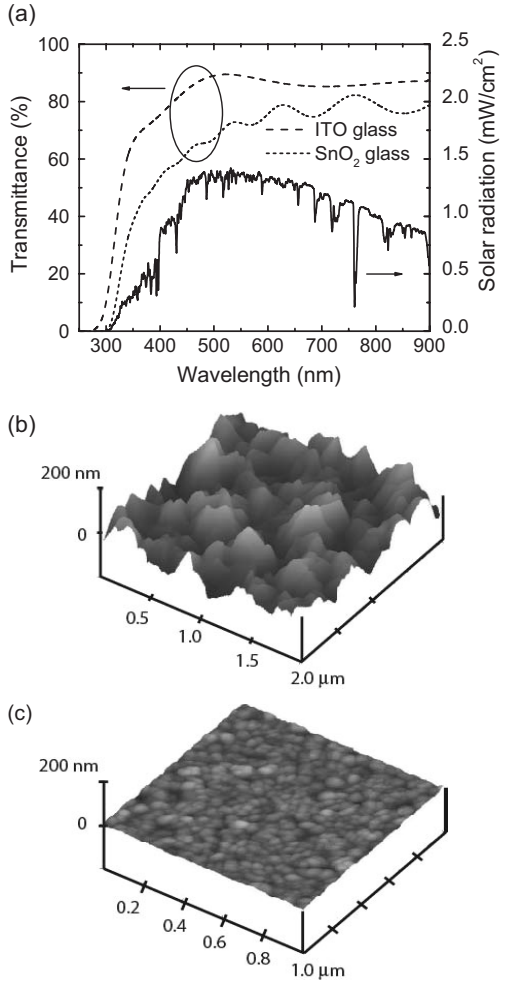

Figure 1. a) Transmittance of SnO_2–F and ITO-coated glass with respect to air mass AM 1.5 solar radiation spectra, and the topography of b) SnO_2–F-coated glass, and c) ITO-coated glass substrates measured using atomic force microscopy (AFM). The root-mean-square surface roughness is 38.7 ± 0.8 nm for SnO_2–F and 2.8 ± 0.6 nm for ITO. The distance between the highest and lowest points (*z*-range) in the scan is 290 nm for SnO_2–F and 27 nm for ITO.

[*] Prof. S. R. Forrest, F. Yang
Department of Electrical Engineering
Princeton Institute for the Science and Technology of Materials (PRISM)
Princeton University, Princeton, NJ 08544 (USA)
E-mail: stevefor@umich.edu
Prof. S. R. Forrest
Departments of Electrical Engineering & Computer Science, Physics, and Materials Science & Engineering
University of Michigan
Ann Arbor, MI 48109 (USA)

[**] The authors thank the National Renewable Energy Laboratory, the Air Force Office of Scientific Research, and Global Photonic Energy Corporation for partial financial support of this work.

of SnO_2–F-coated glass make this material suitable for solar-cell applications.

A comparisons of the surface roughness between the SnO_2–F- and ITO-coated glass substrates is shown in Figure 1b and c, respectively. Cross-sectional scanning electron microscopy (SEM) images (not shown) reveal that SnO_2–F forms large crystals with an average layer thickness of approximately 750 nm, resulting in a surface root-mean-square (RMS) roughness of (38.7 ± 0.8) nm, and a total height variation in a 2 μm × 2 μm area as large as 290 nm (see the atomic force microscopy (AFM) image in Fig. 1b). By comparison, the ITO layer is only 150 nm thick and has a comparatively smooth surface (Fig. 1c) with a RMS roughness of 2.8 ± 0.6 nm and a height variation of 27 nm. The difference in oxide thickness also contributes to the difference in transmittance of the two substrates.

Solar cells with an organic double HJ structure of CuPc(200 Å)/C_{60} (400 Å)/2,9-dimethyl-4,7-diphenyl-1,10-phenanthroline (BCP, 100 Å) and a 1000 Å thick Ag cathode grown on ITO-coated glass using conventional vacuum thermal evaporation (VTE) have been shown to have a power-conversion efficiency of $\eta_p = 3.6 \pm 0.2$ %.[16] In contrast, devices with the same organic layers deposited on SnO_2–F-coated glass show an Ohmic (i.e., non-rectifying) behavior. The rough surface of the SnO_2–F can induce direct contact between the oxide anode and the Ag cathode, thus shorting the CuPc/C_{60} junction. Spin-coating a 200 nm thick 3,4-polyethylenedioxythiophene/polystyrenesulfonate (PEDOT/PSS) planarizing layer[17] on the SnO_2–F surface prior to VTE deposition of the CuPc (200 Å)/C_{60} (400 Å)/BCP (100 Å)/Ag (1000 Å) heterostructure eliminates these shorts, although it introduces additional series resistance, thereby resulting in solar cells with power-conversion efficiencies of less than 0.1 %.

Unlike growth using VTE where the molecules follow radial trajectories from source to substrate, the molecules in OVPD diffuse through a boundary layer before reaching the substrate at random incident angles. Hence, the molecules can diffuse into recesses on rough surfaces that are otherwise unreachable by VTE.[18] Indeed, by changing the OVPD growth conditions for CuPc and C_{60}, we are able to adjust the film surface morphology and crystallization to optimize interfacial surface area while achieving a continuous substrate coverage.[14,18] In this work, three structures with 490 ± 5 Å thick C_{60} acceptor layers are grown on the surface of CuPc donor films on SnO_2–F. In the planar HJ (PHJ) shown in Figure 2a, both CuPc and C_{60} form continuous layers, with a CuPc thickness of 240 Å (d1). In the BHJ structure (d2, Fig. 2b), we first grew a 120 Å thick CuPc layer followed by a layer of CuPc with nanometer-scale protrusions.[18] The average thickness of this second growth was also 120 Å. Structure d3 (Fig. 2c) consists of CuPc protrusions without a continuous base layer. SEM images show a smooth surface consisting of a 240 Å thick continuous CuPc layer as used in structure d1 (Fig. 3a), and a planar-plus-rough CuPc film used in structure d2 (Fig. 3b), where the protrusions evenly distribute on the conformal layer that covers the SnO_2–F crystals. The CuPc

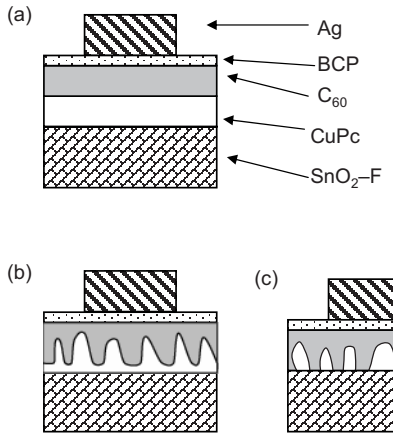

Figure 2. Schematic structures for CuPc/C_{60} solar cells grown on SnO_2–F-coated glass. a) Planar CuPc followed by planar C_{60} layer, b) a continuous CuPc layer with nanometer-sized protrusions covered by a planar C_{60} layer, and c) CuPc nanometer-sized protrusions with no continuous CuPc layer, covered by a planarizing C_{60} layer. Note in structure (c) the C_{60} layer forms conductive pathways between the SnO_2–F anode and BCP/Ag cathode, while such pathways do not exist in structures (a) and (b).

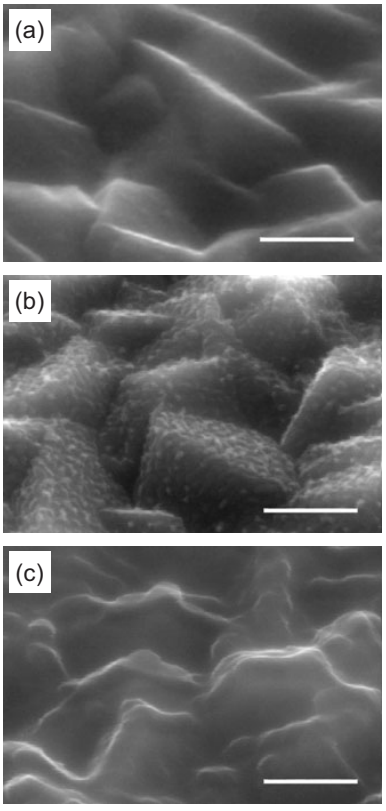

Figure 3. SEM images of the surface morphologies of organic films grown on SnO_2–F using OVPD. a) 240 Å thick continuous CuPc layer, b) 120 Å thick continuous layer followed by a rough CuPc layer, and c) C_{60} layer grown on top of (b). Scale bars in all microscopic images correspond to a distance of 200 nm.

ADVANCED MATERIALS

protrusions are comparable to the exciton diffusion length, L_D, that is, they are 20–30 nm wide and 40–50 nm high. After the CuPc growth, C_{60} is deposited in the same OVPD chamber without exposure to atmosphere. As shown in Figure 3c, C_{60} forms a smooth and planar surface that completely covers the CuPc protrusions in Figure 3b.

All three CuPc/C_{60} HJ devices show rectification in the dark (Fig. 4a), and generate photocurrent under illumination (Fig. 4b), forming solar cells with thin organic layers (< 800 Å) on the rough SnO_2–F substrates. For the PHJ structure d1, and the BHJ structure d2, the current rectification ratios at ±1.0 V in the dark are greater than 10^4, implying a continuous p–n junction between the SnO_2–F anode and the Ag cathode. In contrast, device d3 has a rectification ratio of eight, since gaps between the CuPc protrusions allows C_{60} to directly contact the underlying SnO_2–F, resulting in local shorts (see Fig. 2c).

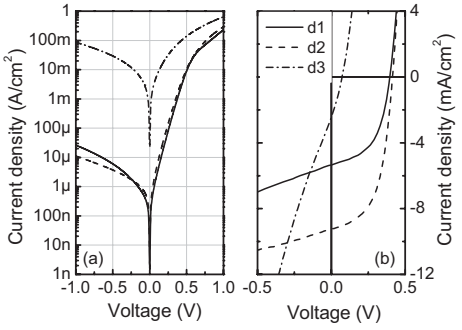

Figure 4. Performance of CuPc/C_{60} solar cells grown on SnO_2–F glass grown using OVPD with different CuPc layers: 240 Å thick continuous CuPc (d1), 120 Å thick continuous layer followed by a protrusive coating (d2), and protrusions without an initial continuous layer (d3). a) Current density–voltage characteristics in the dark, b) current density–voltage characteristics under 1 sun (100 mW cm^{-2}) AM 1.5 illumination.

The performances of the four devices under illumination are compared in Figure 4b. Device d3, with its small shunt resistance, has a small open-circuit voltage (V_{OC} = 0.08 V) and a low fill factor (FF), as expected. The short-circuit current density (J_{SC}) increases from 5.2 mA cm^{-2} in device d1, to 9.1 mA cm^{-2} in the BHJ device, d2. This indicates that the interdigitated CuPc/C_{60} interface is effective in increasing the exciton dissociation efficiency at the D–A junction.

The external quantum efficiency (EQE) was measured as a function of wavelength in Figure 5a. The EQE peaks centered at λ = 620 and 695 nm are due to absorption in CuPc, and the EQE peak at 470 nm is due to the absorption in C_{60} (Fig. 5b). In Figure 5a, the EQE of CuPc at λ = 620 nm increases from 19 % in the PHJ to 31 % in the BHJ, while the peak at λ = 470 nm only increases from 5 to 6 %. This implies that the increase in D–A interface area characteristic of the BHJ is more efficient in dissociating excitons absorbed in CuPc, where the exciton diffusion length of L_D = 10 nm is less than that in C_{60} (L_D = 40 nm[1]). From the overlap integral of EQE(λ) with the AM 1.5 solar irradiation spectrum,[15] we

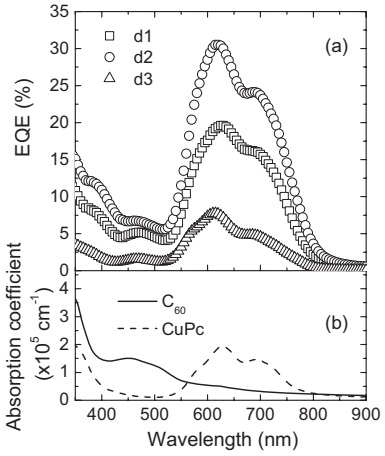

Figure 5. a) EQE of CuPc/C_{60} PV cells grown using OVPD with different HJ structures, and b) absorption coefficient of CuPc and C_{60}.

calculate J_{SC} for the PHJ device (d1) and the BHJ device (d2) to be 3.5 and 6.1 mA cm^{-2}, respectively, or approximately 30 % lower than the values obtained by direct measurement. This is attributed to the device degradation and mismatch between the simulated and standard AM 1.5 solar spectra.[19,20]

The performances of the four CuPc/C_{60} HJ solar cells were further studied by measuring the devices under different illumination intensities. The responsivity (J_{SC}/P_0, where P_0 is the incident light power) is plotted in Figure 6a as a function of P_0. Device d2 has a responsivity of 0.11 ± 0.01 AW^{-1} at 1 sun, a value close to twice of that of d1 (0.060 ± 0.005 AW^{-1}), while the responsivity of d3 is 0.028 ± 0.005 AW^{-1}. In Figure 6b, we find that the FF is greater than 0.5 for the BHJ and PHJ devices when illuminated under the range of 0.02 to 8 suns, and that the FF is greater than 0.55 at 1 sun, implying that the controlled growth of a BHJ does not introduce series resis-

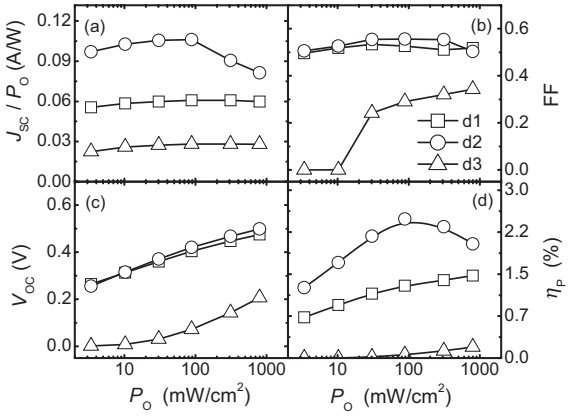

Figure 6. The performance of CuPc/C_{60} solar cells grown on SnO_2–F coated glass grown by OVPD under various light intensities for several HJ structures: a) Responsivity, defined as J_{SC}/P_0, where P_0 is the incident light intensity and J_{SC} is the short-circuit current, b) FF, c) V_{OC}, and d) power-conversion efficiency (η_P).

tance,[18] an advantage over the random BHJ solar cells obtained by mixing polymers[21] or annealing small-molecule D–A mixtures.[22] In addition, V_{OC} is unchanged for devices d1 and d2 across the entire range of intensities shown in Figure 6c, despite their different morphologies. By comparison, V_{OC} of device d3 is lower due to its small shunt resistance, as expected.

The interface area is similar between the BHJ structure d2 and the protrusion-without-continuous-layer CuPc/C_{60} structure (d3), but the increases in responsivity, FF, and V_{OC} in d2 show the importance of having a continuous CuPc layer covering the anode to eliminate current shunt paths. Note that V_{OC} of the PHJ devices grown on SnO_2–F is approximately 0.1 V less than that of a control PHJ CuPc/C_{60}/BCP/Ag device grown on an ITO anode under similar illumination intensities.[23,24] The difference of V_{OC} is comparable to the work function (ϕ) difference between SnO_2–F ($\phi = 4.9$ eV) and ITO ($\phi = 4.8$ eV),[3] although a systematic study of the origin of V_{OC} is beyond the scope of this work.

Figure 6d shows the power-conversion efficiencies of the various CuPc/C_{60} junction devices studied. The BHJ device has the highest η_P, peaking at 2.5 ± 0.2 % at 1 sun illumination, which is twice of that of PHJ device ($\eta_P = 1.3 \pm$ % for d1), and ten times of that of d3, where $\eta_P = 0.6 \pm 0.1$ % at 1 sun. Compared to the previously published PHJ structure ITO/CuPc (200 Å)/C_{60} (400 Å)/BCP (100 Å)/Ag (1000 Å) where $\eta_P = 3.6 \pm 0.2$ %[16] and $\eta_P = 3.2 \pm 0.2$ %[14] grown by VTE and OVPD, respectively, η_P of the cells grown on SnO_2–F in this work is lower, possibly due to the higher resistance of the 750 nm thick oxide, and the non-optimized organic-layer thicknesses.

In conclusion, we have grown efficient small-molecule organic solar cells on indium-free SnO_2–F-coated glass substrates using OVPD, and have studied the influence of nanoscale HJ morphology on the solar-cell performance. We find that the conformal nature of OVPD growth results in continuous layers of CuPc and C_{60} on the rough SnO_2–F surface, resulting in high-efficiency devices. OVPD growth was used to generate either a planar interface, or one with nanoscale features on the order of an exciton diffusion length in CuPc. The BHJ solar cell formed by a continuous layer plus protrusions CuPc and a covering C_{60} layer has a power efficiency of 2.5 ± 0.2 % at 1 sun simulated AM 1.5 G illumination, close to twice of that of similar PHJ devices. Our results show that OVPD can be used to grow efficient organic solar cells on low-cost SnO_2–F-coated glass substrates.

Experimental

Small-molecular-weight organic layers used in the PV cells were deposited using OVPD [14,18] on either commercial SnO_2–F [8] or ITO-coated [25] 1.1 mm thick glass substrates. The SnO_2–F layer was 750 nm thick, and the ITO layer was 150 nm thick. The solvent-cleaned substrates [16] were exposed to UV +O_3 treatment for 5 min immediately prior to loading into the OVPD chamber. Prior to CuPc and C_{60} deposition, the organic materials were purified in three cycles using vacuum thermal gradient sublimation. The OVPD growth chamber (base pressure < 90 mTorr; 1 Torr ≈ 133.3 Pa) maintains a continuous high-purity nitrogen flow through the organic sources [14,26]. The substrate temperature is controlled by flowing water through a copper holder. The N_2 carrier-gas flow rate was regulated with mass flow meters (MKS Instruments) and the chamber pressure was independently controlled with a butterfly valve (MKS Instruments). The conditions for the growth of planar CuPc were: $T_{source} = 446 \pm 1$ °C, $T_{substrate} = 16 \pm 1$ °C, N_2 flow rate = 150 sccm, chamber pressure = 0.587 ± 0.001 Torr, and the deposition time was 140 s. The growth conditions for rough CuPc films were: $T_{source} = 446 \pm 1$ °C, $T_{substrate} = 6 \pm 1$ °C, N_2 flow rate = 100 sccm, chamber pressure = 1.000 ± 0.001 Torr, and the deposition time was 140 s. The growth conditions for C_{60} were: $T_{source} = 472 \pm 2$ °C, $T_{substrate} = 16 \pm 1$ °C, N_2 flow rate = 100 sccm, chamber pressure = 0.460 ± 0.001 Torr, and the deposition time was 830 s. After CuPc/C_{60} growth, the samples were transferred through a nitrogen glove-box into a vacuum chamber with a pressure less than 2×10^{-7} Torr, where a 100 Å thick BCP layer, and the 1000 Å thick Ag cathode were deposited through a shadow mask with an array of 1 mm diameter circular openings using thermal evaporation.

The surface morphologies of SnO_2–F- and ITO-coated glass substrates were studied with an X30 field-emission scanning electron microscope (Philips) and a Dimension 3000 atomic force microscope (Veeco) in tapping mode. A variable angle, spectroscopic ellipsometer (WASE series, J. A. Woollam) was used to measure the thickness of films on the Si wafer to determine the growth rate. Solar-cell performance was tested in ambient conditions in air. Unless otherwise noted, the *J–V* characteristics and power-conversion efficiencies of the devices were measured under simulated AM 1.5G solar illumination at 1 sun intensity using an HP4155B semiconductor parameter analyzer. The illumination intensity was varied using neutral density filters and measured using a calibrated broadband optical power meter. Photocurrent spectra were recorded using a monochromatic beam of light from a tungsten–halogen lamp and chopped at 400 Hz. The monochromatic light was calibrated using a Si photodetector, and photocurrent was measured using a lock-in amplifier referenced to the chopper frequency. Transmittance and absorption spectra were measured using a Perkin–Elmer Lambda 800 UV/vis spectrometer.

Received: April 12, 2006
Final version: May 4, 2006
Published online: July 6, 2006

[1] P. Peumans, A. Yakimov, S. R. Forrest, *J. Appl. Phys.* **2003**, *93*, 3693.
[2] S. R. Forrest, *MRS Bull.* **2005**, *30*, 28.
[3] R. G. Gordon, *MRS Bull.* **2000**, *25*, 52.
[4] T. Jansseune, *Compd. Semicond.* **2005**, *11*, 34.
[5] M. Grätzel, *MRS Bull.* **2005**, *30*, 23.
[6] T. L. Chu, S. S. Chu, C. Ferekides, J. Britt, C. Q. Wu, *J. Appl. Phys.* **1991**, *69*, 7651.
[7] Y. Arai, M. Ishii, H. Shinohara, S. Yamazaki, *IEEE Electron Device Lett.* **1991**, *12*, 460.
[8] Asahi Glass Fabritech Co., Ltd. 3-25-12, Tarumi-cho, Suita-city, Osaka, Japan, 564-0062.
[9] J. C. Bernede, F. Brovelli, S. Marsillac, F. R. Diaz, M. A. Del Valle, C. Beaudouin, *J. Appl. Polym. Sci.* **2002**, *86*, 1128.
[10] A. R. V. Benvenho, J. P. M. Serbena, R. Lessmann, I. A. Hümmelgen, R. M. Q. de Mello, R. W. C. Li, J. H. Cuvero, J. Gruber, *Braz. J. Phys.* **2005**, *35*, 1016.
[11] R. Valaski, R. Lessmann, L. S. Roman, I. A. Hümmelgen, R. M. Q. Mello, L. Micaroni, *Electrochem. Commun.* **2004**, *6*, 357.
[12] R. Valaski, F. Muchenski, R. M. Q. Mello, L. Micaroni, L. S. Roman, I. A. Hümmelgen, *J. Solid State Electrochem.* **2006**, *10*, 24.
[13] M. Baldo, M. Deutsch, P. Burrows, H. Gossenberger, M. Gerstenberg, V. Ban, S. Forrest, *Adv. Mater.* **1998**, *10*, 1505.

ADVANCED MATERIALS

[14] F. Yang, M. Shtein, S. R. Forrest, *J. Appl. Phys.* **2005**, *98*, 014 906.
[15] National renewable energy laboratory, ASTM G-173-03, air mass 1.5 reference solar spectral irradiance. Website: http://rredc.nrel.gov/solar/spectra/am1.5/ (accessed June 2006).
[16] J. Xue, S. Uchida, B. P. Rand, S. Forrest, *Appl. Phys. Lett.* **2004**, *84*, 3013.
[17] P. Peumans, S. R. Forrest, *Appl. Phys. Lett.* **2001**, *79*, 126.
[18] F. Yang, M. Shtein, S. R. Forrest, *Nat. Mater.* **2005**, *4*, 37.
[19] P. Peumans, S. R. Forrest, *Appl. Phys. Lett.* **2002**, *116*, 1713.
[20] S. Yoo, B. Domercq, B. Kippelen, *Appl. Phys. Lett.* **2004**, *85*, 5427.
[21] J. J. M. Halls, C. A. Walsh, N. C. Greenham, E. A. Marseglia, R. H. Friend, S. C. Moratti, A. B. Holmes, *Nature* **1995**, *376*, 498.
[22] P. Peumans, S. Uchida, S. R. Forrest, *Nature* **2003**, *425*, 158.
[23] P. Peumans, V. Bulovic, S. R. Forrest, *Appl. Phys. Lett.* **2000**, *76*, 2650.
[24] S. Khodabakhsh, B. M. Sanderson, J. Nelson, T. S. Jones, *Adv. Funct. Mater.* **2006**, *16*, 95.
[25] Applied Film Corp., 6797—Winchester Circle, Boulder, CO 80 301.
[26] M. Shtein, H. F. Gossenberger, J. B. Benziger, S. R. Forrest, *J. Appl. Phys.* **2001**, *89*, 1470.